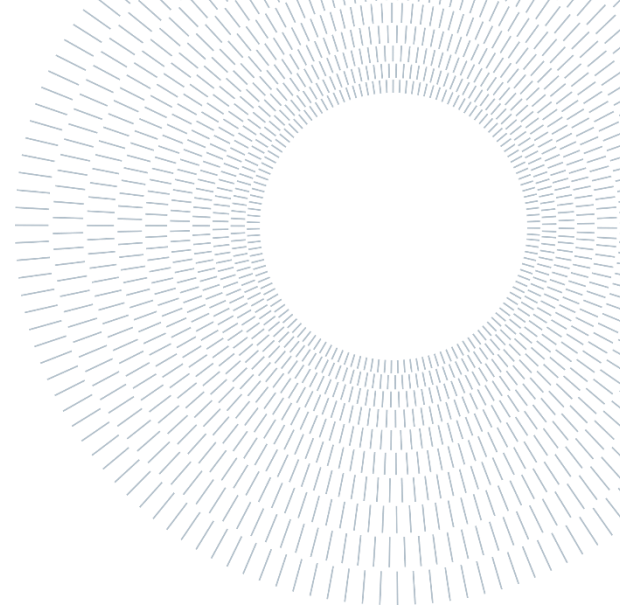




POLITECNICO
MILANO 1863

SCUOLA DI INGEGNERIA INDUSTRIALE
E DELL'INFORMAZIONE



EXECUTIVE SUMMARY OF THE THESIS

Different Sealing Processes for a Plasma Electrolytic Oxidation (PEO) Coating on AA6082

TESI MAGISTRALE IN MATERIALS ENGINEERING AND NANOTECHNOLOGY – INGEGNERIA DEI MATERIALI E DELLE NANOTECNOLOGIE

AUTHOR: MUHAMMAD IBRAHIM ADAM AHMED

ADVISOR: PROF. MARCO ORMELLESE

ACADEMIC YEAR: 2023-2024

1. Introduction

Aluminum alloys of the 6xxx family (Al-Mg-Si) are famous for their lightweight and other good properties such as mechanical, thermal, and electrical properties, as well as corrosion resistance. In almost all neutral environments, they spontaneously generate a passive, stable oxide film that protects the underlying metal from subsequent severe corrosion phenomena. However, this film is thin (a few nanometers thick) and insufficient to ensure passivity in the various fields of aluminum application, especially if the environment is alkaline, acidic, or containing aggressive species.

Plasma Electrolytic Oxidation (PEO) is an emerging plasma-based electrochemical process that allows the creation of a thick oxide layer using high electric potentials and alkaline electrolyte solutions free from harmful substances. During the PEO process, repeated dielectric breakdowns through the growing oxide layer take place in

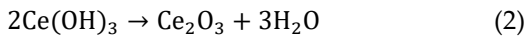
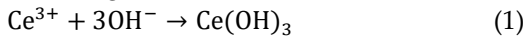
the form of discharges all over the substrate surface. The growth of the oxide coating is attributed to the quenching and collapsing of the molten oxide that is generated during plasma discharges [1].

The structure of the oxide created through PEO is notably porous, due to the plasma discharges that occur during the process along with the liberation of gases. Therefore, it is necessary to seal those pores to hinder the passage of corrosive species. Some of the sealants could have two-fold effects, not only physically blocking the pores, but also providing inhibiting phenomenon for active corrosion protection.

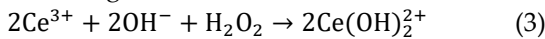
This work aims to fine-tune the electrical parameters for obtaining a thicker oxide layer and to compare some immersion sealing methods performed on AA6082 substrates treated with PEO. Mainly cerium nitrate and in-situ synthesis of LDH (Layered Double Hydroxide) structure sealings were performed.

The first one was **cerium nitrate sealing**. Cerium is characterized by two oxidation states (Ce^{3+} , Ce^{4+}). These cations, through hydration reactions, lead to the formation of a stable, insoluble cerium-rich layer that is composed of cerium oxides/hydroxides. The precipitation of cerium oxides/hydroxides at the interface between the anodic oxide film and the sealing solution, and then into the pores can occur due to the rise of pH value. At first, by immersing the anodic film into the cerium-based solution it partially dissolves. Then due to the local pH rise, the precipitation of cerium oxides/hydroxides begins. H_2O_2 is used in the treatment solution to accelerate the transformation of Ce^{3+} to Ce^{4+} . The precipitation of cerium oxide/hydroxide is promoted via two pathways. The first is through Ce(III), present in the initial Ce(III) nitrate solution (Eq. 1, 2), and the second is through Ce(IV) species (Eq.3-6). The second pathway can only occur in the presence of H_2O_2 .

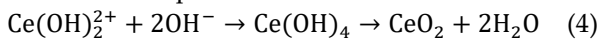
Concerning the Ce(III) pathway, the precipitation of cerium compounds proceeds according to the following reactions:



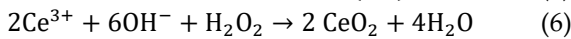
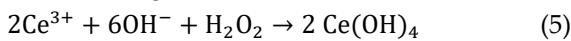
For the Ce(IV) pathway, initial oxidation of Ce(III) takes place in the presence of H_2O_2 according to the following reaction:



Subsequently, and for a higher pH, the following reaction takes place.



Other reactions where Ce^{3+} ions can be directly oxidized to Ce(IV) compounds in the H_2O_2 -containing solution without passing through the $\text{Ce}(\text{OH})_2^{2+}$ intermediate are possible according to the following reactions:

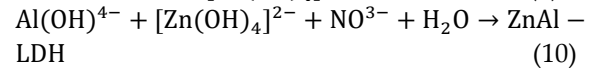
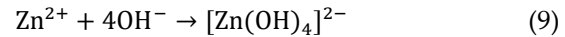
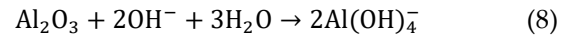
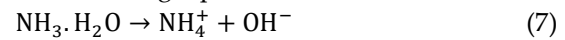


The control of the pH plays a vital role in the formation of the desired cerium-rich layer [2].

The other sealing treatment was **LDH (Layered Double Hydroxide) sealing**. In general, layered double hydroxides are represented by the formula $[\text{M}_{1-x}^{2+}\text{M}_x^{3+}(\text{OH})_2]_n^+ [\text{A}^{n-}]_m \cdot n\text{H}_2\text{O}$, where M^{2+} are divalent cations and M^{3+} are trivalent metal cations. "A" refers to the n-valent anions. The LDH structure is formed when M^{2+} is replaced by M^{3+} and A^{n-} anions being intercalated in the interlayers

of LDHs to balance the net positive charge, and the molar ratio of $\text{M}^{3+}/(\text{M}^{2+} + \text{M}^{3+})$ is in the range 0.20 to 0.33. Because of the anion exchange capability of LDHs, different anions can be intercalated inside the LDH interlayer to change its chemistry for specific applications. Nitrate anion (NO_3^-) possesses one of the lowest values of ion exchange equilibrium constant, hence, it can be easily substituted by another anion e.g. anti-corrosion inhibitor (VO_x^-).

LDH films are formed on a PEO substrate by an in-situ growth process. In this process, almost all the micropores and cracks in the PAO film can be sealed due to the precipitation of the LDH inside them. Moreover, the corrosion resistance of the substrate materials can be further improved by intercalating corrosion inhibitors or hydrophobic agents inside the interlayers of the LDH film. The ZnAl-LDH formation process can be illustrated by the following equations:



Sealing the anodized aluminum substrate with LDHs provides significant active and passive corrosion protection. LDHs can provide active corrosion inhibition by entrapping the aggressive species from the corrosive medium in the interlayers, and through the self-healing properties of LDHs [2],[3],[4],[5].

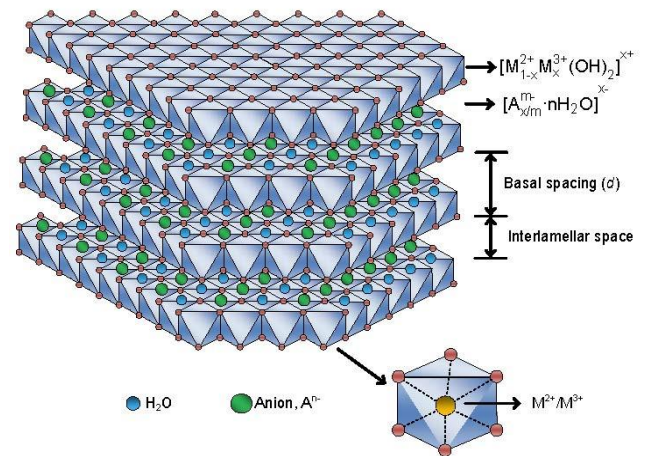


Figure 1. A schematic representation of the LDH structure.

2. Materials and methods

The experimental procedures were carried out on specimens of AA6082 disks having circular sections, with diameter $D = 10$ mm and thickness $t = 5$ mm.

2.1 PEO

For the PEO process, an alkaline electrolytic solution with the composition reported in Table 1 was used.

Table 1. Electrolytic solution for the PEO process.

Composition	Concentration
KOH	11.22 g/L ⁻¹ (0.2 M)
Na ₂ SiO ₃	7 g/L ⁻¹
NaAlO ₂	3 g/L ⁻¹
C ₃ H ₈ O ₃ (glycerin)	10 g/L ⁻¹

California Instruments Asterion 751 series AC/DC was used as a power source. It was working in a potential-controlled AC regime. The chosen waveform was 60A%-40C%-7CP%. The frequency was set at 1000 Hz. The selected potential values were reached through a constant ramp and then maintained constant. A multi-step process was applied, with the parameters reported in Table 2.

Table 2. PEO process parameters

Voltage type	Sweep time (s)	Plateau time (s)	Voltage (V)
Voltage sweep	60	120	324
Voltage drop	0.00025	60	-
Voltage sweep	60	120	350
Voltage drop	0.00025	60	-
Voltage sweep	60	180	376
Voltage drop	0.00025	120	-
Voltage sweep	60	120	389

2.2 Sealing

Sealing processes were performed by immersing the PEO-treated samples in 150 mL of sealing solution. The temperature was monitored and kept constant using an IKA magnetic stirrer with a heating plate (mod. C-MAG HS 7) and thermocouples. Moreover, the solution was continuously stirred at 100 rpm using a magnetic anchor to prevent temperature gradients and ensure homogeneity.

Regarding **cerium nitrate**, a treatment bath of cerium nitrate was prepared using deionized water as a solvent and 6.51 g/L of Ce(NO₃)₃·6H₂O. The bath was heated to the treatment temperature (37°C) and was kept constant during the processing time (30 min). When the set temperature was reached, the PEO-coated samples were immersed in the bath for the whole treatment time. At the end of the treatment, all the sealed samples were rinsed with distilled water and dried in nitrogen. Table 3 summarizes the parameters of cerium nitrate sealing treatment. The cerium nitrate-treated PEO samples are labeled as Ce-S.

Table 3. Cerium nitrate sealing parameters.

Sealing solution	Concentration (M)	Temperature (°C)	Sealing time (min)
Ce(NO ₃) ₃	0.015	37	15

LDH sealing is a two-step sealing treatment. The first step is the sealing, and the second step is the ion exchange process. The first step is to seal the pores and cracks of the PEO-coated samples by forming ZnAl-LDH with NO₃⁻ incorporated in the interlayers. The second step though for exchanging the NO₃⁻ anions with the corrosion inhibitor VO₃⁻ anions and hence the final LDH will be ZnAl-LDH intercalated with VO₃⁻ in the interlayers.

At first, a solution of zinc nitrate was prepared using deionized water as a solvent and 14.87 g/L of Zn(NO₃)₂·6H₂O. The bath was heated to the treatment temperature (90°C) and was kept constant during the processing time (15 min). When the set temperature was reached, the PEO-coated samples were immersed in the bath for the whole treatment time. At the end of the treatment, all the sealed samples were rinsed with distilled

water and dried in nitrogen. Then the second step was performed by immersing the dried treated samples in a bath of sodium vanadate. The bath was prepared by using deionized water as a solvent and adding 12.13 g/L of NaVO_3 . Then it was heated to the treatment temperature (50°C) and was kept constant during the processing time (15 min). At the end of the treatment, all the sealed samples were rinsed with distilled water and dried in nitrogen. Table 4 summarizes the parameters of LDH sealing treatment.

Table 4. LDH sealing parameters.

Step	solution	Conc. (M)	Temp. ($^\circ\text{C}$)	Time (min)
#1	$\text{Zn}(\text{NO}_3)_2$	0.05	90	15
#2	NaVO_3	0.1	50	15

2.3 Characterization Analyses

For the microscopy analysis a Carl Zeiss EVO 50VP SEM, equipped with a Bruker X-ray spectrometer (EDS) for chemical microanalysis was employed. Unfortunately, the X-ray diffractometer (XRD) was out of order during the period of this work.

2.4 Electrochemical Analyses

The electrochemical analyses were carried out using a Metrohm Autolab PGSTAT with a standard three-electrode cell, consisting of the investigated sample as working electrode, a pre-calibrated silver/silver chloride (SSC) reference electrode, and a platinum net as counter electrode. For all tests, the sample was immersed in 200 mL of NaCl 0.35 wt.% solution, using a PTFE (Teflon) tape for covering and insulating the junction part of the sample so that only 3 cm^2 was exposed to the aggressive solution. The tests were conducted at room temperature.

For EIS analysis, a range of frequencies between $10^5 - 10^{-2}\text{Hz}$ was applied. A sinusoidal signal

was employed, with an amplitude of $0.01\text{ V}_{\text{RMS}}$, collecting 10 points per decade of frequency.

Potentiodynamic polarization analyses were performed with a scan rate of $10\text{ mV}\cdot\text{min}^{-1}$. The sample polarization was $\pm 0.3\text{ V}$ with respect to the open circuit potential (V_{OCP}).

3. Results and discussion

The results obtained from both the microscopical investigations and electrochemical tests are discussed in this section.

3.1 Characterization Tests Results

The image of the surface of PEO-base is reported in Figure 2.

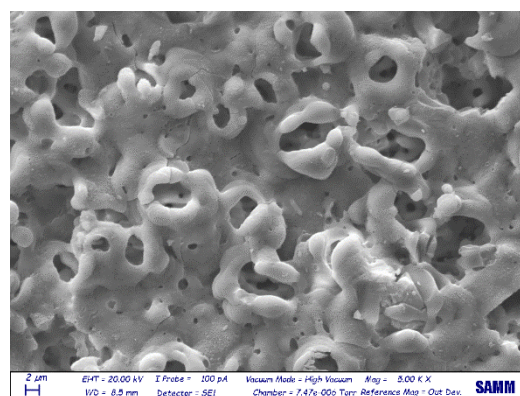


Figure 1. SEM image of PEO base surface with 5000x magnification.

The surface morphology shows a uniformly distributed microporosity, with crater-shaped pores. Along with some microcracks around the pores. Porosity is attributed to the micro-discharge channels formed during the PEO process, whereas microcracks are due to the relaxation of thermal stresses produced by significant temperature gradients and phase transitions occurring during the PEO process.

The EDS map of the PEO-base surface (figure 3) confirms the presence of elements from both the substrate and the electrolyte in the developed oxide, as expected.

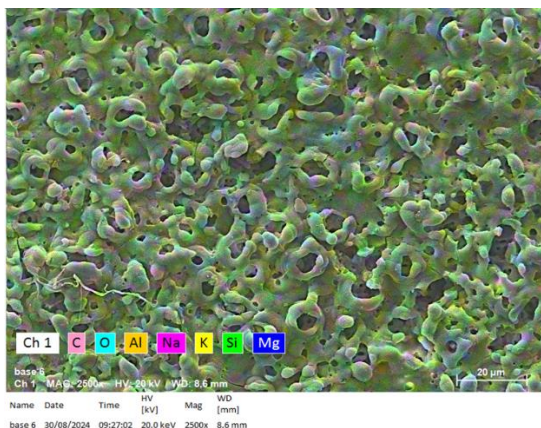


Figure 2. EDS map of the unsealed PEO surface.

The average thickness of the coating was measured using a cross-sectional SEM micrograph of a Ce-S sample and found to be 17.37 μm (figure 4). The morphology of the cross-section exhibits a wavy behavior on the surface and at the interface with the substrate. Which is due to the mechanism of the oxide layer formation. Moreover, from the cross-sectional image, the three distinct layers of a PEO coating can be realized; the thin compact barrier layer, the intermediate dense layer, and the porous outer layer.

A surface micrograph instead revealed that the morphology of the Ce-S surface is quite similar to that of the PEO-base. The EDS map did not exhibit any other elements different than those in the PEO-base. However, as will be discussed in the electrochemical results part, the Ce-S showed a promising corrosion resistance performance.

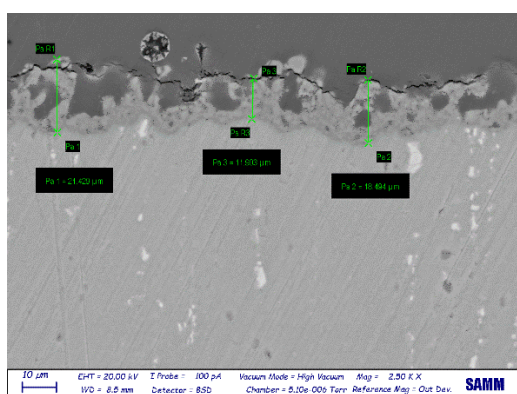


Figure 4. SEM micrograph of the cross-section of Ce-S at a magnification of 2500x.

For what concerns the LDH-S, the SEM micrograph of the surface showed a similar morphology to that of the PEO-base. Instead, the EDS map of the surface revealed other elements along with those in the PEO-base. Mainly zinc and vanadium, coming

from the sealing treatment as shown in Figure 5. Even though the well-known LDH nanocontainer flakes on the surface are unseen, one can hypothesize that they are at the very first nucleation stage and hence are invisible.

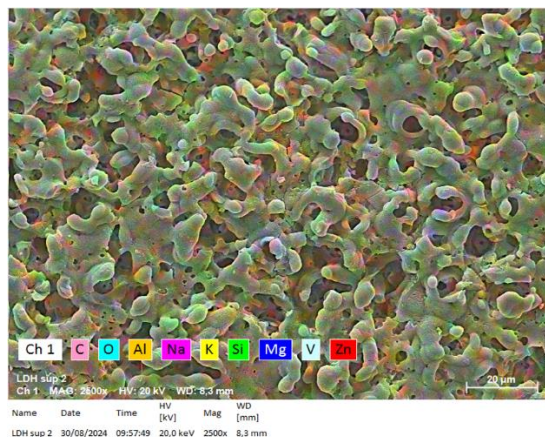


Figure 5. EDS map of Ce-S surface.

3.2 Electrochemical Impedance Spectroscopy (EIS) Results

Nyquist diagrams of PEO-base, Ce-S, and LDH-S are reported in Figure 6, with an enlargement of the PEO-base using a different scale, for clarity.

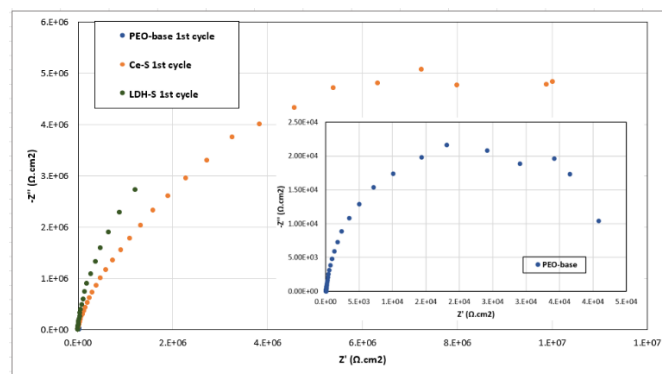


Figure 3. Nyquist diagrams of PEO-base, Ce-S, and LDH-S.

Both types of sealing greatly improve the corrosion resistance performance of the coated samples as manifested by the increase in the impedance values by three orders of magnitude with respect to the unsealed PEO sample. The Nyquist curves of both Ce-S and LDH-S exhibit a single incomplete semicircle, indicating a strong resistive behavior to charge transfer reactions. For Ce-s the protective behavior is quite stable in time as it is indicated by an almost overlap of the curves of the three

immersion cycles (figure 7); however, it is not the case for LDH-S. The obtained polarization resistance values for the three systems are reported in Table 6.

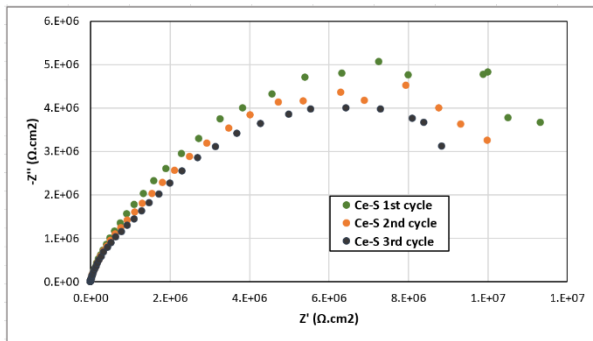


Figure 4. Nyquist diagrams of Ce-S for the three immersion cycles.

Table 6. Polarization resistance values obtained through Nyquist plots for the three systems.

Sample	R_p ($\Omega.cm^2$)
PEO base	4.4466×10^4
Ce-S	1.4432×10^7
LDH sealed PEO	1.0858×10^7

3.3 Potentiodynamic Polarization Curves

Potentiodynamic polarization curves of all three systems (PEO-base, Ce-S, and LDH-S) along with the bare AA6082 are shown in a summary plot in Figure 8. Through this plot, it can easily be observed that the PEO coating only slightly improves the corrosion protection of the bare alloy, whereas both the sealing treatments significantly increase the corrosion resistance of the PEO coating and hence the bare alloy.

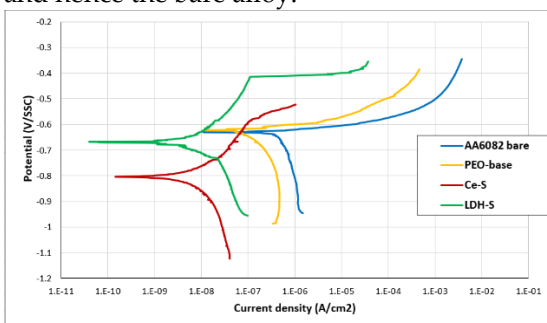


Figure 8. Summary plot of potentiodynamic polarization curves.

Both Ce-S and LDH-S exhibit a more negative corrosion potential (E_{corr}) compared to PEO-base, however, they reduce the corrosion current density (i_{corr}) by three orders of magnitude; a tremendous enhancement in corrosion resistance behavior. The more negative corrosion potential could be attributed to various factors, such as temperature, experimental conditions, and the surface state of the specimen. However, it was reported in the literature for the LDH sealing treatment that it could be due to the inhibitory effect of the corrosion inhibitor associated with this sealing treatment (vanadate anions). It is worth noting that the obtained results from the analysis of the potentiodynamic polarization curves are in agreement with those obtained from the other electrochemical tests. A summary table reporting all the extrapolated corrosion parameters is reported in Table 7.

Table 5. Summary table of potentiodynamic polarization parameters.

Sample	E_{corr} (V _{SCE})	i_{corr} (A·cm ⁻²)
AA 6082	-0.6296	$9.2513 \cdot 10^{-6}$
PEO base	-0.6219	$5.51 \cdot 10^{-6}$
Ce-S	-0.8029	$9.2663 \cdot 10^{-9}$
LDH-S	-0.6677	$7.8983 \cdot 10^{-9}$

4. Conclusions

Many different electrolytes and electrical parameters of the PEO process were tried and modified to fine-tune the properties of the resulting oxide coating for corrosion resistance applications, mainly composition, compactness, and thickness.

Despite all the effort put into fine-tuning the electrolyte and electrical parameters, the produced PEO coating contained a high amount of porosity, which makes it vulnerable to corrosion. Porosity is

an intrinsic feature of PEO coatings attributed to the mechanism of their formation. Hence sealing treatments were necessary.

Two sealing treatments were selected for their demonstrated high corrosion resistance performance and environmental friendliness, cerium nitrate and layered double hydroxide (LDH). The sealed PEO samples were investigated using SEM, EDS, and electrochemical tests (EIS, LPR, and PDP). The sealed PEO samples showed a significant improvement in corrosion resistance compared to the unsealed one even though the microstructural and elemental composition investigations did not show the expected results.

Therefore, superior corrosion resistance performance is expected in case the sealing products are fully developed, indicating the outstanding protective behavior of the chosen treatments. Thus, more work is needed to optimize the conditions for the complete development of the expected sealing treatments' products. For example, increasing the treatment time, fine-tuning the composition of the solution, and adjusting the treatment temperature.

Impedance and polarization resistance (R_p) measurements showed a significant enhancement in the case of the sealed samples. R_p was higher by three orders of magnitude for both treated samples with respect to the unsealed PEO sample. Thus, manifesting the high opposition of the treated samples to polarization and corrosion phenomena. However, the cerium-nitrate treated sample showed much better stability of the protective behavior over time.

Both cerium-nitrate- and LDH-treated PEO samples showed corrosion potentials (E_{corr}) more negative than the unsealed sample, for the LDH the difference was less. However, they both exhibit corrosion current densities lower by three orders of magnitude than those of the unsealed ones, proving the effectiveness of the sealing treatments. Further studies and investigations are required to first optimize the PEO process for obtaining a coating with a minimal amount of porosity possible, and then optimize the sealing treatments for the complete formation of the sealing products with the hope of not only sealing the opening of the pores, but even inside the pores and thus providing the best corrosion protection.

Bibliography

- [1] **Soumya Sikdar, Pramod V. Menezes, Raven Maccione, Timo Jacob and Pradeep L. Menezes**, « Plasma Electrolytic Oxidation (PEO) Process— Processing, Properties, and Applications- A review», *Nanomaterials*, *Nanomaterials* 2021, 11, 1375. <https://doi.org/10.3390/nano11061375>.
- [2] **Muhammad Ahsan Iqbal, Luyi Sun, Allyson T. Barrett and Michele Fedel**, « Layered Double Hydroxide Protective Films Developed on Aluminum and Aluminum Alloys: Synthetic Methods and Anti-Corrosion Mechanisms», *Coatings* 2020, 10, 428; doi:10.3390/coatings10040428.
- [3] **Yingdong Li, Songmei Li, You Zhang, Mei Yu, Jianhua Liu**, « Enhanced protective Zn–Al layered double hydroxide film fabricated on anodized 2198 aluminum alloy», *Journal of Alloys and Compounds*, 630 (2015), 29–36, <http://dx.doi.org/10.1016/j.jallcom.2014.12.176>.
- [4] **M. Serdechnova, M. Mohedano, M. Kuznetsov, B. Mendis, C.L. Starykevich, M. Karpushenkov, S. Tedim, J.Ferreira, M.G. Blawert, C. Zheludkevich**, «PEO coatings with active protection based on in-situ formed LDH-nanocontainers», *J. Electrochem. Soc.* 2017, 164, C36–C45.
- [5] **B. Kuznetsov, M. Serdechnova, J. Tedim, M. Starykevich, S. Kallip, M. P. Oliveira, T. Hack, S. Nixon, M. G. S. Ferreirac, and M. L. Zheludkevich**, «Sealing of tartaric sulfuric (TSA) anodized AA2024 with nanostructured LDH layers», *RSC Adv.* 2016, 6, 13942–13952.